31st Annual International Conference of the IEEE EMBS
Minneapolis, Minnesota, USA, September 2-6, 2009

Cell tracking in fluorescence images of embryogenesis processes with morphological reconstruction by 4D-tubular structuring elements

D. Pastor, M. A. Luengo-Oroz, B. Lombardot, I. Gonzalvez, L. Duloquin, T. Savy,
P. Bourgine, N. Peyrieras and A. Santos

Abstract— **We present a simple and parameter-free nuclei tracking method for reconstructing cell dynamics in fluorescence 3D+t images of embryogenesis. The strategy is based on the use of the mathematical morphology operators directly in the 4D image. The morphological reconstruction of a marker - manually or automatically selected- in an initial spatio-temporal position generates a connected path over the time representing the cell migration. Thus, the processing provides a coherent spatio-temporal estimation of cell movement. The algorithm has been validated on *in vivo* images of early zebrafish and sea urchin embryogenesis acquired with two-photon laser scanning microscopy providing mean tracking rates above 98% per time step.**

I. INTRODUCTION

In the recent years, we have witnessed how multidisciplinary approaches to biological sciences are being combined in order to integrate high-throughput biological data provided by new technologies [1]. Several works are oriented to integrate massive bioimaging data, encouraging the development of image acquisition and analysis techniques to reach the automatic observation of cells morphodynamics [2]. One of the new objectives of these integrative approaches is to obtain spatio-temporal descriptions of the regulatory processes at the cell level. Fluorescence microscopy techniques allow us to obtain *in vivo* images of embryogenesis. Two-photon, confocal and scanned light sheet [3] microscopy have been successfully used to image such processes in several vertebrate and invertebrate organisms. Image analysis is therefore critical to reconstruct embryogenesis processes. Different computer vision paradigms have been applied for this purpose, but because of the lack of standardized acquisition protocols and the heterogeneity of the data, image processing and analysis in the context of cell morphodynamics remains an open challenge [4][5]. The analysis of embryogenesis morphodynamics usually consists in an initial pre-processing step, secondly, in the registration and segmentation of the cells in the different 3D volumes and, finally, in the estimation of the movement by linking cells detected in different time-steps [6]. Complex algorithms based on deformable models and active contours are a powerful strategy for segmenting cells [4]. Optical flow techniques to extract vector fields [7] enhance the results of tracking methods by establishing prior positions inferred from the previous time step [8]. The major disadvantages of these techniques is that they are highly computational expensive and, as they require to identify cells in each 3D image and estimate the movement *a posteriori*, they may introduce an uncontrolled source or errors at the nuclei detection step then turned into errors in the cells trajectory and lineage.

The proposed algorithm tracks cells in 3D+t images which do not need to segment the cells but works directly in the 4D space-domain [9], finding connected paths over time as 4D tubular shapes. The reconstruction of the cell trajectories starts from a selected individual marker in a spatio-temporal position and provides its individual backward tracking. The flexibility in the marker creation allows us to easily track just a preferred set of cells during a particular period of the dataset. We embedded the algorithm in an application featuring options to trigger customized tracking, visualize results in several modes and correct them. The algorithm has been validated in the reconstruction of the early embryogenesis of the zebrafish (*Danio rerio*) and the sea urchin (*Paracentrotus lividus*). Both of them are widely used animal models because of the complete transparency of their embryo and their representative phylogenetic positions. Their nuclei have been highlighted with a fluorescent protein that allows time-lapse imaging with two-photon laser scanning microscopy.

This article is organized as follows. In section 2 we introduce the basic morphological reconstruction and the 4D structuring element. The tracking method is described in section 3 while section 4 shows some experimental results and their validation. Finally, discussion closes the article.

II. MATHEMATICAL FOUNDATIONS

A. Morphological operators

The basic morphological operators are dilation $\delta_B(f(x)) = \sup_{y\in B}\{f(x-y)\}$ and erosion $\varepsilon_B(f(x)) = \inf_{-y\in B}\{f(x-y)\}$. These two elementary operations can be composed in opening $\gamma_B(f) = \delta_B[\varepsilon_B(f)]$ and closing $\varphi_B(f) = \varepsilon_B[\delta_B(f)]$. Morphological *openings* (*closings*) filter out light (dark) structures from the images according to the predefined size and shape criterion of the structuring element. *Area opening* is a particular connected

This work is supported by the European projects Embryomics (NEST 012916) and BioEmergences (NEST 028892) and the joint research project Spain-France MORPHONET (HF2007-0074).

D. Pastor, M. A. Luengo-Oroz, I. Gonzalvez and A. Santos are with the Group of Biomedical Image Technologies, ETSIT, Universidad Politcnica de Madrid, Avnda. Complutense 30, Madrid 28040 Spain. {david.pastor, maluengo, andres}@die.upm.es

L. Duloquin and N. Peyrieras is with DEPSN, CNRS, Institut de Neurobiologie Alfred Fessard, Gif-sur-Yvette 91190, France. nadine.peyrieras@inaf.cnrs-gif.fr

B. Lombardot, T. Savy and P. Bourgine are with CREA-Ecole Polytechnique, Paris 75015, France. paul.bourgine@polytechnique.edu

978-1-4244-3296-7/09/$25.00 ©2009 IEEE

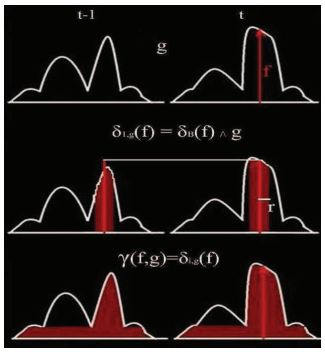

Fig. 1. Example of a 4D morphological backward reconstruction. (Top) Mask in white (g) and marker in red (f) (Middle) First geodesic dilation of f by a backward structuring element with radius r. The marker is dilated generating two regions of radius r in t and t-1 with the marker intensity (thanks to the backward kernel). Then, a geodesic comparison of the dilation and the mask image limits the histogram. (Bottom) Reconstructed image in t and t-1 from the marker in t.

operator based on the notion of surface area [10]. The grey tone area opening of f of size λ_a, denoted $\gamma^a_{\lambda_a}(f)$, is given by: $\gamma^a_{\lambda_a}(f)(\mathbf{x}) = \sup\{h \leq f(\mathbf{x}) \mid A(\gamma^c_{\mathbf{x}}(X_h(f))) \geq \lambda_a\}$, where $A(X)$ is the area of X. The area opening can be seen as an opening with a structuring element which locally adapts its shape to the image structures.

The morphological *reconstruction by dilation* [11] (Fig. 1) is implemented using the *geodesic dilation* operator based on restricting the iterative dilation of a function marker f by B (a structuring element) to a function mask or reference g, $\delta^n_g(f) = \delta^1_g\delta^{n-1}_g(f)$, where $\delta^1_g(f) = \delta_B(f) \wedge g$ is the intersection. The *reconstruction* by dilation is defined by $\gamma^{rec}(g,f) = \delta^i_g(f)$, such that $\delta^i_g(f) = \delta^{i+1}_g(f)$ (idempotence).

B. 4D Structuring elements

In order to perform morphological operators directly in the 4D image, a 4D structuring element has to be defined. Instead of using a 4D ball structuring element ($r^2 = x^2+y^2+z^2+t^2$), we have chosen a 4D tubular structure that corresponds to a 3D ball that remains still in time (Fig. 2a). A similar concept of spatio-temporal connectivity has been previously used in [12], where 4D line segment structuring elements have been used for noise removal in time-lapse images of zebrafish embryo membranes. Tubular backward kernels allow us to reconstruct the nuclei region in past time steps within a maximum shift (the radius of the tube) as shown in Fig. 1. By backtracking the cell we establish connected paths over the time as shown in Fig. 2b.

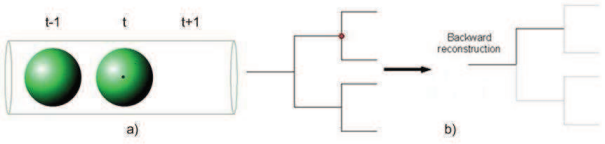

Fig. 2. a) 4D backward tube b) Time connected paths generated by a)

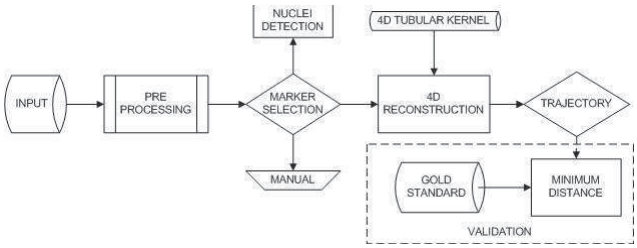

Fig. 3. Cell backtracking algorithm workflow

III. METHODS

A. Overview

First, we implement a light pre-processing module. Then, we select either automatically, or manually the markers of the cells to track (tracking is performed individually). The filtered image is used as a mask for the 4D reconstruction process based on the tubular kernel. Individual trajectories are obtained from the reconstructed 4D image by analyzing each 3D frame. The resulting workflow is shown in Fig. 3.

B. Pre-processing

Input images are pre-processed with a median filter and thresholded for low level noise values. Due to the heterogeneous illumination in depth for zebrafish images we also apply a 3D area top-hat to remove noise forming big connected components: $f' = (f) - \gamma^{\upsilon_2}_B(f)$.

C. Nuclei Detection

As it has been drafted before, this is an optional stage: either we manually select the cells to be tracked, either we perform an automatic detection and detected cells are followed. The automated detection is performed for the time step we trigger the backtracking method. The pre-processed image is filtered with a 3D area opening by the minimal size allowed for nuclei regions υ_1. Therefore, $f'' = \gamma^{\upsilon_1}_B(f')$. The local maximum values of f'' -which are flat zones of size υ_1- are selected as a rough segmentation of nuclei and consequently as markers for the backtracking algorithm. This method can be tuned to obtain low rates of false positives for an easier validation procedure.

D. Cell Backtracking

We use a 4D tube structuring element that defines the spatio-temporal connectivity. The morphological reconstruction is applied in the 4D volume until reaching a reconstructed region that covers the maximum possible shift of the nucleus. The output 4D image features a single maximum which contains the marker and corresponds to the spatio-temporal reconstructed migration of the cell (see Fig.4). Thus, in each 3D frame the region that is spatio-temporally connected to the initial marker is highlighted. Trajectory points correspond to the maximum of the reconstructed volume and are extracted backwards in time starting from the marker. In case several maxima are found in a 3D frame (corresponding with a cell with two mother cells when backtracking - which is biologically impossible), the closest

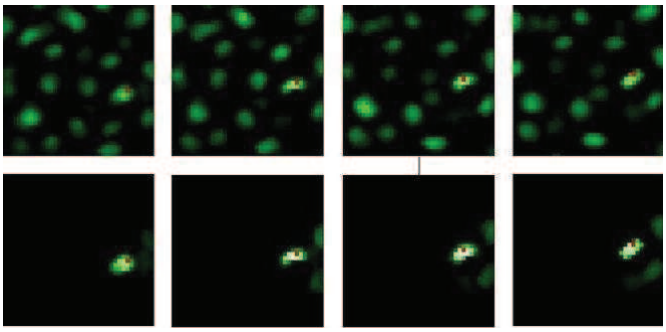

Fig. 4. Upper row: Four consecutive pre-processed images. Lower Row: Reconstructed output of the filtered images from the initial spatio-temporal marker. Red points indicates the reference of the manually extracted trajectory used for validation

maximum to the last point of the trajectory is selected for the sake of coherence. Each cell is reconstructed individually and the lineage is produced by merging *a posteriori* two cells with a common sub-trajectory. The computation of the trajectory is totally low-cost compared to a segmentation/tracking approach. Detection and backtracking results are validated in the next section.

E. Implementation

This work has been implemented in C++ using the Insight ToolKit framework [1] and the Mathematical Morphology contributions to the framework [13] [14]. The choice of this framework has been encouraged for several reasons. This is an open-source framework, template-based, strongly typed and with standard naming conventions which makes easy its distribution and re-usability. It also features interesting technical details such as pipeline-processing models, multi-threading and the capability to process specific regions of the same image in parallel.

IV. RESULTS

We tested our method with two different datasets. Results are validated using a *Gold Standard* (GS) of manually corrected nuclei centers in a specific sub-volume of the embryo along ten time consecutive steps for each dataset.

A. Zebrafish dataset

Time-lapse images of zebrafish embryogenesis were obtained through time-lapse two-photon laser scanning microscopy. A wild type zebrafish egg was injected with mRNA encoding fluorescent protein H2B/mcherry (red fluorescent protein staining nuclei). Images were acquired from 4 hours post fertilization with the z-axis going from the animal to the vegetal pole. Data have an isotropic spatial resolution of $1.37\mu m$ and a temporal resolution of 67 seconds. The evaluation is restricted to the GS boundaries (459 cell trajectories).

1) Nuclei Detection: We have tested the nuclei detection module over the zebrafish dataset. The goal is to provide a robust detection of nuclei centers (less than 5% of false positives FP) while still detecting most of them (OK) to use them as markers for backtracking. Best results were obtained for υ_1=30 (76% OK, 4% FP) and υ_1=40 (70% OK, 2% FP). This parameter and υ_2 values were tuned heuristically. They characterize the minimum and maximum nuclei size at this stage of the embryo development.

2) Cell Backtracking: We have backtracked 459 cells of the GS along 11 consecutive images -longer trackings would be performed iteratively setting the last extracted center as the new marker as we also need to reset the reconstruction level which may decrease in each time step (see Fig. 1.)- Validation against the GS trajectories is performed in the same way for both datasets. We applied the Euclidean distance to the GS trajectory points of each cell to define an acceptance region for the corresponding tracking, so the obtained trajectory is valid only if all of its points fall within that region. The radius of the acceptance region depends on the image parameters (r=6 pixels for this dataset).

Results in Fig. 5 show the ratio of tracked nuclei per time step. We can observe very high rates of correctly tracked (98.1% on average) nuclei per step (nps) and the performance is constant along the ten steps. This reflects the uniform evolution of the embryo at this stage.

Even obtaining these satisfactory rates, algorithm could perform better with finer imaging techniques. Furthermore, errors can be explained theoretically. The remaining 2% of lost nps are candidates might be influenced by mitosis. Depending on the time-step between two images, the shift of daughter cells with respect to the mother can be too large for the structuring element to connect the nuclei. In this critical situation, the reconstruction operator will connect the closest neighbor nucleus creating a 4D connected path following other trajectory. Otherwise, if there is no nucleus close enough, the reconstruction signal will be lost and the tracking will require to be reset selecting a new marker.

B. Sea urchin dataset

Data of the live early sea urchin embryo is acquired using the same microscopical imaging technique and injecting the embryo at the one cell stage with the same red protein encoding RNA for nuclei staining. Extracted 3D images have a $0.48x0.48x0.96\mu m$ voxel size and a time-step of 2 min and

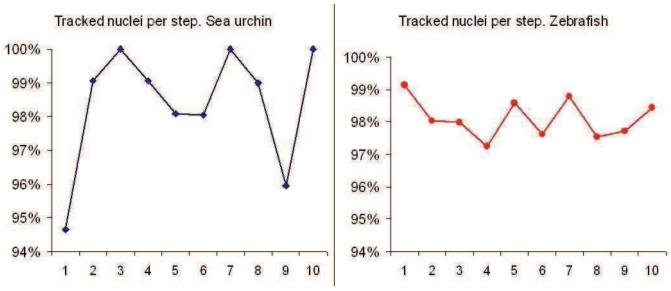

Fig. 5. Percentage of well tracked cells per time step

[1] http://www.itk.org/

13 seconds starting 5h45min post fertilization. At this stage, the embryo features big cells and well isolated nuclei moving slowly between images. The radius for the acceptance region is 15 pixels.

1) Cell Backtracking: We backtracked all the cells of the embryo present in the last frame of the dataset (112) till the first frame to get insight about the embryo dynamics during this period. This dataset allowed better performance of our algorithm as the reconstruction operator found less interconnected nuclei (more isolated shapes) and the shifts after mitosis could be filled (slower motion). The average of tracked cells per step (see Fig. 5) is 98.4%, better than the obtained value for the zebrafish dataset confirming our conclusions. However, the tracking rate decreases sharply to 95% rates in some steps as the embryo is moving because of its cilia. The global nucleus shift produced by the cell movement and the organism displacement makes the reconstruction operator track other nucleus generating a false mitosis when reconstructing the whole lineage.

C. Integration

The algorithm has been embedded in the Morphogenesis Visualization Tool (MOVIT) capable of displaying data in several modes: raw data, nuclei centers, trajectories or lineages (see Fig. 6). Both, automatic nuclei detection or manual nuclei selection can be used for triggering the method. It also allows us to manually correct results and make annotations. Along with the tracking, the algorithm returns confidence values based on the intensity profile of the reconstructed image per step. When the reconstruction operator can barely connect the shift of the nuclei along time, the reconstruction signal decreases significantly meaning that a possible mitosis or a global displacement occurred. Thus, the user can check out the situation and select the next marker on the real trajectory to achieve a whole successful tracking and reconstruct the migration and lineage of the target cells.

V. CONCLUSIONS AND FUTURE WORK

We have introduced a simple, flexible and fast algorithm for cell backtracking based on the novel concept of 4D structuring elements that identifies moving cells with 4D tubular shapes. The algorithm has been validated in zebrafish and sea-urchin time-lapse images. It provided very good results with minimal dependence on the target dataset (quality of images or organism). Due to its simplicity the algorithm improves its performance in presence of images with a short time-step and well isolated nuclei shape. Limitations of the algorithm due to the imaging techniques can be partially solved by using some extra light modules (filtering and trajectory estimation).

Complex structuring elements as large backward tubes that reconstructs more than one past step or spatio-temporal horns which cover greater volume in past steps are being tested with promising results. These kernels can be used as complement of the simple tubular kernel to reconstruct trajectories where a nucleus is too corrupted in a particular image or the shift after a mitosis is too large to be filled. In this sense, forward tracking strategies are also being implemented. Future work also includes optimizations to achieve almost real-time tracking of manually selected cells.

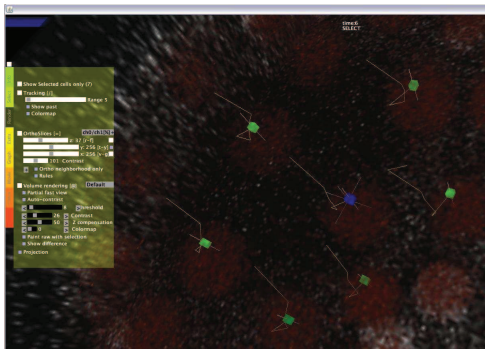

Fig. 6. Display of nuclei trajectories over raw data rendering.

VI. ACKNOWLEDGEMENTS

We specially thank the zebrafish and the sea-urchin teams for their great effort in producing tracking data used for this work, and all the members of the projects Embryomics, BioEmergences and MorphoNet for our fruitful multidisciplinary interaction.

REFERENCES

[1] H. Peng, "Bioimage informatics: a new area of engineering biology," *Bioinformatics*, vol. 24, no. 17, p. 1827, 2008.
[2] S. Megason and S. Fraser, "Imaging in systems biology," *Cell*, vol. 130, no. 5, pp. 784–795, 2007.
[3] P. Keller, A. Schmidt, J. Wittbrodt, and E. Stelzer, "Reconstruction of zebrafish early embryonic development by scanned light sheet microscopy," *Science*, vol. 322, no. 5904, p. 1065, 2008.
[4] C. Zimmer, B. Zhang, A. Dufour, A. Thebaud, S. Berlemont, V. Meas-Yedid, and J. Marin, "On the digital trail of mobile cells," *IEEE Signal Processing Magazine*, vol. 23, no. 3, pp. 54–62, 2006.
[5] E. Meijering, I. Smal, and G. Danuser, "Tracking in molecular bioimaging," *IEEE Signal Processing Magazine*, vol. 23, no. 3, pp. 46–53, 2006.
[6] O. Drblikova, M. Komornikova, M. Remesikova, P. Bourgine, K. Mikula, N. Peyrieras, and A. Sarte, "Estimate of the cell number growth rate using PDE methods of image processing and time series analysis," *Journal of Electrical Engineering*, vol. 58, no. 7, pp. 86–92, 2007.
[7] B. Lombardot, M. Luengo-Oroz, C. Melani, E. Faure, A. Santos, N. Peyrieras, M. Ledesma-Carbayo, and P. Bourgine, "Evaluation of four 3d non rigid registration methods applied to early zebrafish development sequences," in *MIAAB MICCAI*, 2008.
[8] C. Melani *et al.*, "Tracking cells in a live zebrafish embryo," in *IEEE Engineering in Medicine and Biology Society*, 2007.
[9] I. Gonzalvez, "4d morphological reconstruction for cell tracking in microscopy images of zebrafish embryogenesis," Master's thesis, Kungliga Tekniska Hogskolan, Sweden, 2008.
[10] L. Vincent, "Morphological area openings and closings for grey-scale images," *Shape in Picture: Mathematical Description of Shape in Grey-level Images*, pp. 196–208, 1993.
[11] ——, "Morphological grayscale reconstruction in image analysis: Applications and efficient algorithms," *IEEE Transactions on Image Processing*, vol. 2, no. 2, pp. 176–201, 1993.
[12] M. Luengo-Oroz, E. Faure, B. Lombardot, R. Sance, P. Bourgine, N. Peyrieras, and A. Santos, "Twister Segment Morphological Filtering. A New Method for Live Zebrafish Embryos Confocal Images Processing," in *IEEE ICIP*, 2007, pp. 253–256.
[13] R. Beare, "Grayscale morphological attribute operations," *Insight Journal*, 2007.
[14] G. Lehmann, "Label object representation and manipulation with ITK," *Insight Journal*, 2008.